2-4 Ultra-Stable Cryogenically Cooled Sapphire-Dielectric Resonator Oscillator and Associated Synthesis Chain for Frequency Dissemination

Clayton R. Locke, KUMAGAI Motohiro, ITO Hiroyuki, NAGANO Shigeo, John G. Hartnett, Giorgio Santarelli, and HOSOKAWA Mizuhiko

A cryogenic sapphire oscillator (CSO) first constructed at the University of Western Australia has been in operation at NICT since 2007. We firstly describe the construction techniques and development of this high performance secondary frequency standard that has repeatedly achieved fractional-frequency fluctuations below 6×10^{-16} at integration times between 10 and 200 s. Secondly, we describe the synthesis chain that down-converts the 11 GHz output of the CSO to 1 GHz for laboratory distribution. The short-term frequency stability of the down-converter itself is better than 1×10^{-15} at an averaging time of 1 second. The long-term drift of the CSO is suppressed by referencing this down-converted signal to a hydrogen maser linked to Japan Standard Time. For microwave-frequency atomic interrogation in the NICT cesium fountain a 9.192-GHz up-converter was developed.

Keywords
Cryogenic sapphire oscillator, Secondary frequency standard, Frequency dissemination, Synthesis chain

1 Introduction

The performance of a primary frequency standard is often limited by the stability of the reference, be it a hydrogen maser or voltage-controlled crystal oscillator. In fact, the frequency stability of the NICT cesium atomic fountain NICT-CsF1 is limited by that of the hydrogen maser[1]. Similarly, the performance of the NICT optical frequency comb is limited by the stability of the repetition rate locked to the hydrogen maser[2]. To overcome these limitations, NICT has introduced a cryogenic sapphire oscillator (CSO), developed in University of Western Australia (UWA) having a short-term frequency stability of about 100 times better than that of the hydrogen maser. By using this ultra-stable source as a flywheel, the performance of the frequency standards developed in NICT can be improved.

The CSO project was inspired by the early work of Braginsky et al. at Moscow State University[3] and the subsequent development at UWA resulted in the creation of microwave signal sources with short-term frequency stability unmatched by any other type of electromagnetic oscillators[4]. The first generation CSOs exhibited a fractional frequency stability close to one part in 10^{14} over integration times of 10–300 s[5]. This was improved by more than an order of magnitude by the mid-1990s when the noise mechanisms affecting the CSOs became better understood[6]. The improvements in the CSO's frequency stability were assisted by the technological advances in growing ultra high-purity single-crystal sapphire via the heat exchange method HEMEX,[7] the availability of low-noise microwave compo-

nents, and the cryogenic operation of the vital components of the oscillator. This oscillator was the first to reach fractional-frequency stability less than one part in 10^{15} over integration times of 10–100s. In 2000, a UWA sapphire oscillator was used at Observatoire de Paris for the development of a laser-cooled cesium-fountain clock. These experiments enabled the first experimental observation of the quantum projection noise in atomic-fountain clocks[8]. In 2003, researchers at UWA and the Paris Observatory teamed up to undertake a search for the possible violations of Lorentz invariance by comparing the frequency of that CSO to that of a hydrogen maser[9]. Also in 2003, another CSO was delivered to European Space Agency CNES to assist with the ground tests of the cold atom space clock "PHARAO" intended to operate in a microgravity environment[10]. In 2005, at UWA a novel type of Michelson–Morley experiment involving two co-rotating CSOs was implemented to test the Lorentz invariance principle under the standard model extension framework and put the best limits on several Lorentz violating parameters. Between 2004 and 2006, four additional CSOs were developed at UWA having fractional-frequency fluctuations of 5×10^{-16} at an integration time of 20 s and highly reproducible over long measurement time periods[11] and having phase noise of −85 dBc/Hz at 1 Hz on a 10 GHz carrier.

Over the past 15 years, in an effort to reduce the running cost of CSOs, various techniques have been tried to raise the temperature at which the resonator has a frequency-temperature turnover point[12]-[15] and also increasing the fraction of impurities in sapphire to raise the compensation point[16] to solid nitrogen temperatures (50 K). Such oscillators having increased losses in the doped resonator and operating at an elevated temperature could never rival the noise performance of liquid-helium-cooled sapphire oscillators.

Recent work[17] has reported on the closing gap between the performance of the CSO and microwave generation from ultra-stable lasers based on optical cavities with very high finesse and extremely low sensitivities to temperature and vibration. An all optical-fiber approach (making use of two erbium fiber mode-locked lasers phase locked to a common ultra-stable reference) generates an 11.55 GHz signal with residual frequency instability of the optical-to-microwave division process of 2.3×10^{-16} at 1s. The absolute microwave frequency stability[18] from two independent ultra-stable optical references exhibits an Allan deviation about 3×10^{-15} at 1 s integration time.

In this paper we describe the development and operation of the CSO at NICT that operates at 11.2 GHz. In order to make the most of this highly stable signal for several experiments in several locations it was necessary to develop synthesis chains to change the oscillation frequency of the CSO to the appropriate frequency without any drastic degradation of the frequency stability of the synthesized signal[19][20]. At first, for the purpose of laboratory distribution, we developed a synthesis chain to down-convert from 11.2 GHz to 1 GHz. This 1 GHz signal is distributed to other experimental rooms via coaxial cable. For dissemination of the 1 GHz signal to distant sites, an optical fiber link is used[21][22]. Additionally, we have assembled a 9.192 GHz synthesis chain for microwave interrogation of the Cs atoms in the NICT cesium fountain CsF-1.

2 Cryogenic sapphire oscillator

At the heart of the CSO is a cylindrical sapphire dielectric resonator with its rotational axis aligned with the crystal axis. Eigenmodes of such a resonator are hybrid and feature all six components of the electromagnetic field. From a broad continuum of the eigenmodes, only two families of quasi-TM and quasi-TE modes are of practical importance to the design of ultrastable oscillators. These modes exhibit the highest field confinement to the dielectric and hence the highest electrical Q-factors. They are characterized by a small number of field variations along the axial and radial directions and a large number of field maxima around the azimuth, which is typical for modes characterized as 'whispering gallery' (WG), similar to

acoustic modes observed by Rayleigh[23]. A WG mode in a cylindrical dielectric resonator is a standing wave formed by a pair of traveling waves counter-propagating along the inside circumference of the dielectric cylinder and experiencing total internal reflection at the dielectric/air interface. Small geometrical imperfections of the sapphire cylinder, the presence of the coupling probes, as well as the misalignment of the crystal and rotation axes remove the degeneracy between the traveling wave "companions" and split the modes of resonance into two spectral doublets having different coupling coefficients with frequencies separated by a few kilohertz. This effect is easily observed at cryogenic temperatures, where the frequency separation between the doublets can be a few hundred times larger than their individual resonance line-widths. A competition between doublets has never been observed in a loop oscillator due to the nonlinearity of its gain stage. Oscillations always establish at the frequency of one of the doublets with the lower insertion loss, which saturate the loop microwave amplifier.

Enclosing the sapphire cylinder in a metal cavity protects it against the environmental perturbations and, most importantly for cryogenic applications, against surface contamination. This also reduces the required size and cost of the sapphire crystal relative to the size and cost of an open-space sapphire resonator tuned to the same frequency. One drawback of the sapphire loaded cavity (SLC) resonator is the relatively high density of spurious cavity-like modes, which may interact with the operational mode reactively or resistively[24][25]. This problem can be solved by cutting a few radial and azimuthal slots in the cavity lids to intercept the flow of microwave currents and cause radiative loss of energy of the spurious modes.

The *Q*-factors of the fundamental WG modes are not affected by the radiative slots, as their energy is almost entirely confined to the interior of the dielectric. In the absence of crystal defects and surface contamination, the *Q*-factors of the WG modes in SLC resonators

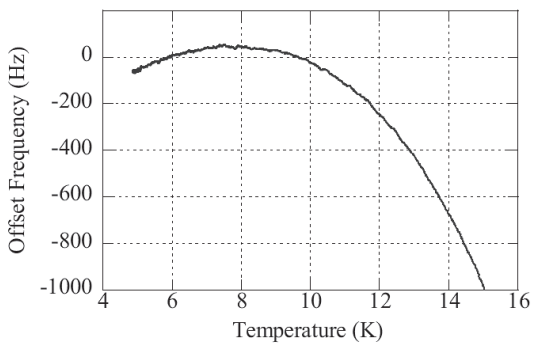

Fig.1 *Frequency-temperature dependence of an 11.9 GHz WGE mode, measured by beating against another CSO and logging the difference frequency as the temperature of one sapphire resonator is ramped.*

are limited by the sapphire-dielectric loss tangent (tanδ). At temperatures 50<T<80 K, the loss tangent is a very strong function of temperature, i.e., tan$\delta \propto T^5$. This trend, however, does not hold at lower temperatures where crystal imperfections reduce the temperature dependence of the microwave losses. Even the highest quality sapphire crystals grown by the HEMEX method exhibit tan$\delta \propto T$ over the temperature range of 2–12 K. Nonetheless, the *Q*-factors measured in the liquid-helium-cooled HEMEX-sapphire resonators at frequencies around 10 GHz are extremely high, of the order of 10^9 at T=4.2 K, with the highest measured *Q*-factor of 1.8×10^{10} at 1.8 K[26].

Even the highest quality HEMEX sapphires are not free from paramagnetic impurities such as Cr^{3+}, Fe^{3+}, Ti^{3+}, or Mo^{3+} ions. In such resonators, the paramagnetic ions, with only a small measurable effect on the *Q*-factor, strongly influence the frequency-temperature dependence of the WG modes by introducing a magnetic susceptibility to the sapphire crystal. The sign of the frequency shift resulting from the temperature induced change in the magnetic susceptibility is opposite to the frequency shift resulting from the temperature dependence of the sapphire-dielectric permittivity. With the magnitudes of the competing frequency shifts becoming comparable below 15 K, frequency-temperature compensation is observed in CSO resonators. Such phenomena exist in all WG

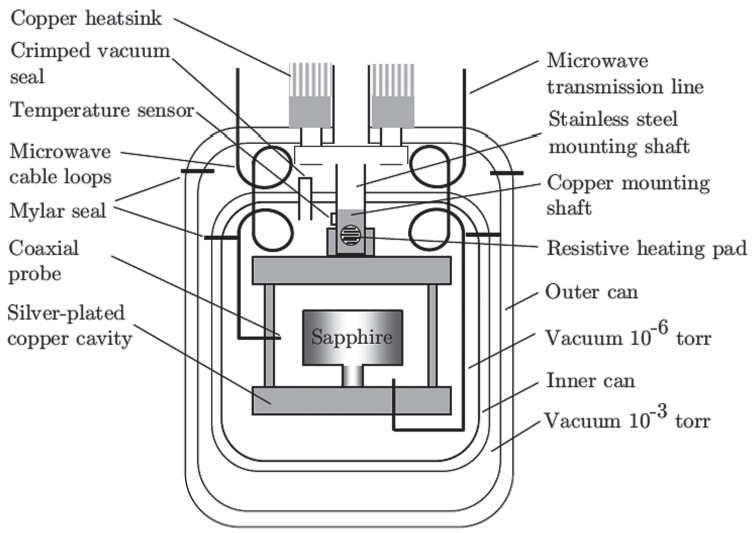

Fig.2 *Schematic diagram showing design features of the lower portion of the helium Dewar insert comprising two vacuum cans and the sapphire loaded cavity*

modes in HEMEX resonators at frequencies below the electron spin resonance frequency, which for Mo^{3+} ions is equal to 165 GHz.

Figure 1 shows the frequency-temperature dependence of a 50 mm diameter, 30 mm high sapphire cylinder, supporting 11.9 GHz excitation in the fundamental WG transverse electric mode. It is this turning-point characteristic that defines these slightly doped sapphire samples as an excellent choice on which to base ultra-stable oscillators. As the exact location of the frequency-temperature maxima depends on the concentration of paramagnetic impurities, their species type, and the nature of the mode excited, some HEMEX sapphires are unsuitable for application to a CSO, having a turning-point temperature either too high or too low. Also, the curvature of the frequency-temperature maximum in the vicinity of the turning point is an important parameter of the resonator, as it determines the required precision of the resonator temperature control. It is defined as $\kappa = (1/f_0)d^2f/dT^2$, where d^2f/dT^2 is the second derivative of the resonance frequency as a function of temperature and f_0 is the mean resonance frequency. In HEMEX-crystal resonators, the smallest values of the fractional curvature are measured around $\kappa = 10^{-9}$ K^{-2}. This can be translated into a resonator fractional-frequency stability of order of 10^{-16}, provided that the crystal temperature is kept within 1 mK of the turning point and the temperature fluctuations are controlled to be less than 0.1 mK. These conditions are not difficult to meet for liquid-helium-cooled resonators due to the availability of high-sensitivity low-noise carbon-glass temperature sensors.

Figure 2 illustrates a typical approach to the temperature stabilization of a cryogenic CSO resonator. The sapphire crystal is thermally insulated from the liquid helium bath by two evacuated stainless-steel vacuum cans. The temperature of the CSO resonator is stabilized to a precision of about 10 μK by a feedback control system based on a temperature bridge connected to a four-terminal carbon-glass thermometer. The latter is embedded into the copper mounting shaft, to which the CSO resonator is directly attached. The top end of the copper shaft is connected to a stainless steel rod to ensure effective low-pass filtering of thermal fluctuations resulting from the boiling liquid helium. The outer can houses multiple microwave isolators which are needed to minimize the CSO resonator frequency pulling effect induced by the coaxial cable line resonances. Amplitude detectors, used in both the frequency and power control systems, are also

located inside the outer can in the cryogenic environment to improve the oscillator's long-term frequency stability. The CSO resonator in Fig. 2 is a single-spindle single crystal sapphire cylinder clamped from below. This type of clamping was suggested in Ref. [27]. to reduce mechanical stress on the active region of the sapphire resonator where most of the electromagnetic field is confined. Such stress was found to be responsible for the frequency drift of the first generation CSOs utilizing double-spindle sapphire cylinders squeezed between the lids of the metal cavity.

3 Noise mechanisms

Three major noise mechanisms limit the frequency stability of the CSO when it operates at the frequency-temperature turning point. The first noise mechanism is intrinsic fluctuations of the Pound frequency discriminator, associated with voltage noise in the detectors and technical fluctuations in the electronics of various feedback control circuits[28][29]. The second noise mechanism is associated with AM-index fluctuations of the microwave interrogation signal incident on the resonator. The third noise mechanism is related to fluctuations of dissipated microwave power in the sapphire resonator due to radiation pressure induced expansion in a solid dielectric resonator[30]. The effect of the first two noise mechanisms on the spectral purity of the oscillator's signal can be greatly reduced by setting the CSO primary coupling close to critical. Such tuning, however, may require a few iterations cool down cycles due to the errors associated with the measurements of very small coupling coefficients and the strong dependence, near 4.2 K, of sapphire Q-factor on its surface cleanliness. In practice, the coupling must be set close to 10^{-4} at room temperature in order to obtain critical coupling at liquid-helium temperature.

In principle, microwave oscillators can be constructed at relatively high cryogenic temperatures (40–80 K) by making use of the simultaneous excitation of both whispering gallery transverse magnetic and transverse electric modes in the same SLC resonator[12][13]. The anisotropy of sapphire permits the cancellation of the temperature dependence of the difference frequency between the two modes when the ratio of the two modes' resonance frequencies $f_{WGE}/f_{WGH} \cong \alpha_{\parallel}/\alpha_{\perp}$, where $\alpha_{\parallel}$ and $\alpha_{\perp}$ are fractional temperature coefficients of sapphire-dielectric permittivity parallel and perpendicular to the crystal axis, respectively. For X-band CSO resonators cooled with liquid nitrogen $\alpha_{\parallel}/\alpha_{\perp}=1.34$, this is equivalent to a mode separation of 3–4 GHz. The fractional-frequency stability of such a dual-mode oscillator operating at 40–50 K has been measured to be 4×10^{-14} over an integration time of 1 second[31]. This is adequate as a flywheel pump oscillator for less demanding experiments, but they cannot approach the noise performance of liquid-helium-cooled sapphire oscillators.

Figure 3 shows a schematic diagram of the oscillator loop of CSO, where the high-Q sapphire resonator serves both as a band-pass filter of a self-sustaining loop oscillator and a dispersive element of a Pound frequency discriminator (FD). Operation of the Pound FD is based on rapid phase modulation (PM) of the incident microwave signal. If the oscillator frequency is different from that of the high-Q resonator the signal reflected from the resonator acquires amplitude modulation (AM), the depth and the phase of which depend on the relative detuning between the oscillator and the resonator. By extracting the complex amplitude of the reflected signal with an envelope detector and comparing it to the original modulation signal (inside a lock-in amplifier as shown), an error voltage synchronously varying with the oscillator frequency is produced.

The filtered error voltage is then applied to the voltage controlled phase (VCP) shifter in the loop oscillator steering its frequency to the chosen resonant mode of the high-Q resonator. The frequency discriminator, filter, and VCP form a closed loop frequency control system which detects and cancels (within its bandwidth) fluctuations of the oscillator frequency from the cavity resonance frequency. For a frequency control loop with the sufficiently high

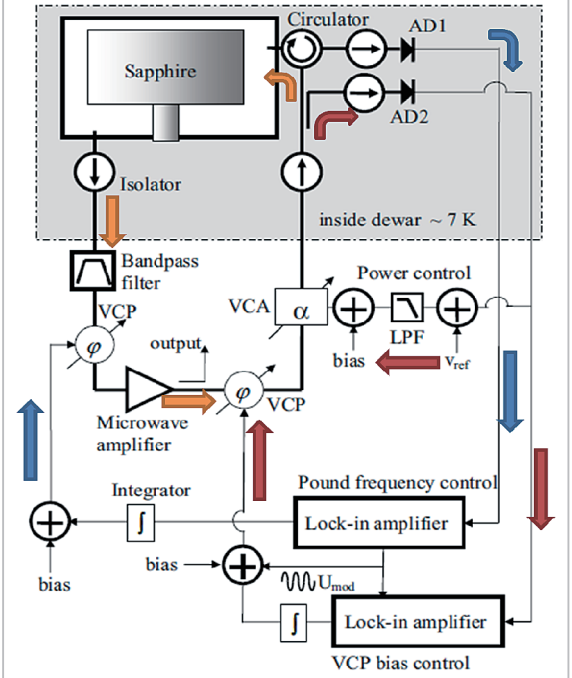

Fig.3 *Schematic diagram of a CSO showing three control systems stabilizing its frequency and power and eliminating the spurious amplitude modulation of the interrogation signal*

Thick lines indicate microwave coaxial cables. VCP=voltage controlled phase shifter, VCA=voltage controlled attenuator, LPF=low pass filter.

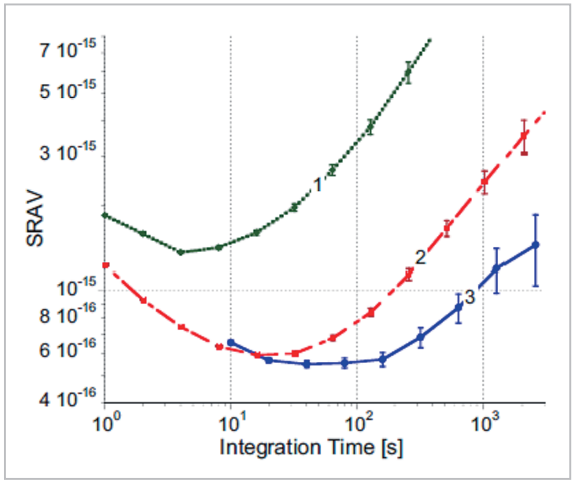

Fig.4 *Measured Allan deviation for a single oscillator from the beat between two nominally identical cryogenic sapphire oscillators*

One oscillator acted as a reference oscillator with all control systems operational. In the second oscillator power control and AM-index suppression was turned off (curve 1: gate time 1 s), power control on, and AM index off (curve 2: gate time of 1 s) and both power control and AM-index suppression on (curve 3: gate time of 10 s).

gain, the quality of oscillator frequency stabilization is entirely determined by the noise properties of the frequency discriminator. To ensure a reliable and efficient operation of the Pound frequency control system, the frequency of phase modulation must be correctly chosen. First of all, it should exceed the bandwidth of the high-Q resonator. This minimizes the loss of the modulation sidebands inside the resonator and improves the discriminator's frequency-to-voltage conversion efficiency. This also eliminates the spurious zero crossings in the dependence of the error voltage on frequency. Such zero crossings may "confuse" the control system into locking the oscillator at a frequency far from the cavity resonance, which would be accompanied by enhanced phase noise due to the reduced value of the discriminator conversion efficiency.

Microwave power incident on the cryogenic sapphire resonator needs to be stabilized in order to minimize power induced frequency shifts associated with the radiation pressure effect. The magnitude of this effect increases with the Q-factor of the resonator, and for high quality HEMEX sapphire resonators (with Q-factors around 10^9) it has been measured to be about 5×10^{-11}/mW[30]. The largest variations of microwave power incident on the SLC resonator are due to the gradual boil off of liquid helium, which changes the loss in the transmission lines connecting the cryogenic resonator to the oscillation sustaining stages. The power control system of a CSO is based on a cryogenic amplitude detector placed as close as possible to the sapphire resonator and a voltage controlled attenuator VCA located in the room temperature part of the loop oscillator next to the phase modulator. Finally, a temperature control system maintains the resonator temperature near the frequency-temperature turning point to ensure a first order immunity of the

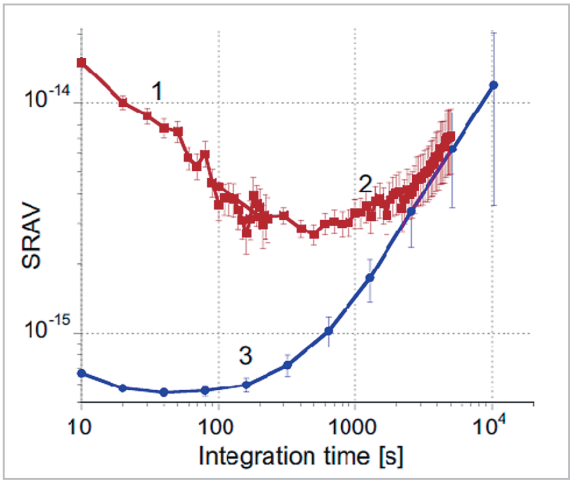

Fig.5 *Measured Allan deviation for a single oscillator from the beat between two nominally identical cryogenic sapphire oscillators (curve 3: gate time of 10 s) and between one cryogenic sapphire oscillator and a hydrogen maser (curve 1: gate time of 10 s; curve 2: gate time of 100 s) to determine the long-term performance*

resonance frequency to ambient temperature fluctuations. Detailed analysis of these noise mechanisms can be found in Ref. [32].

To evaluate the short-term stability, two almost identical CSOs operating at 11.2 GHz were constructed. In each oscillator, the temperature of the CSO resonator was maintained at its frequency-temperature turning point near 7 K with a commercial temperature controller by using a carbon glass thermometer as a temperature sensor. The beat frequency between the two oscillators ($f$beat=131.181 kHz) was measured with a frequency counter referenced to a hydrogen maser. The fractional frequency uncertainty of the measurement system was limited by the counter triggering errors and is a diminishing function of the integration time: $\sigma_y^{\text{count}} \cong 10^{-16}/\sqrt{\tau}$

The effect of switching off various control systems on the noise properties of the CSO is illustrated by measurements in Fig. 4. It shows the importance of having the power stabilization and AM-index suppression systems for reaching the good long-term frequency stability of the oscillator.

Figure 5 shows the Allan deviation of the fractional-frequency fluctuations of the CSO at NICT (σ_y) as a function of integration time, reaching a minimum σ_y^{min} 5.6×10^{-16} at $\tau = 20$ s and remaining below the level of 10^{-15}. In addition to inter-comparison of two CSOs, we also compared the beat between the CSO and a hydrogen maser. As expected, the maser noise dominates the noise measurements at the relatively short integration times (τ<2000 s) , while at larger integration times, the results of both experiments very well agree with each other.

The values of σ_y were directly calculated from the raw data without any post-processing such as a removal of the linear frequency drift typical for the earlier oscillators. This was due to the extremely low drift rates exhibited by the oscillators. Such performance, we believe, was due to the optimal geometry of the shielded sapphire resonator characterized by a relatively sparse spectrum of spurious modes in the vicinity of the operational one. The NICT CSO is maintained in a temperature-controlled room (±0.2°C) and other than two brief periods of maintenance, it has been kept at or below 77 K for over four years. Over this time the drift has been continually monitored and is approximately 10^{-14} /day.

4 Frequency down-conversion

In order to use the CSO signal for several experiments in other rooms at NICT, we have developed a synthesis chain to down-convert from 11.2 GHz to 1 GHz. Figure 6 shows the block diagram of the 1 GHz down-converter. The output signal of a 1 GHz low-noise surface acoustic wave (SAW) oscillator is amplified and injected into a nonlinear transmission line. The nonlinear transmission line is used for frequency multiplication as a frequency comb generator. The 11th harmonic (11 GHz) is band-pass filtered and mixed with the 11.2 GHz output from the CSO to generate a 200.5 MHz signal. The 5th harmonic (5 GHz) from another nonlinear transmission line is divided to 208.3 MHz by divide-by-eight and divide-by-three prescalars. The 208.3 MHz signal is mixed with the 200.5 MHz to generate 7.8 MHz. Fine tuning of the down-converter is achieved by con-

trolling a commercial direct digital synthesizer (DDS) in the chain. To avoid stability degradation due to the DDS it has modified to take its external reference from a 40 MHz signal generated from the 1 GHz signal of the SAW oscillator through two divide-by-five stages. The zero beat between the two 7.8 MHz signals at the last mixer is used to phase-lock the 1 GHz SAW oscillator to the CSO. The relation between the output frequencies of the CSO, the DDS and the SAW is given by,

$$CSO - \left(11 + \frac{5}{24}\right) \cdot SAW = DDS$$

Consequently, the 1 GHz signal is controllable with a resolution of about 0.1 μHz maintaining the stability of the CSO.

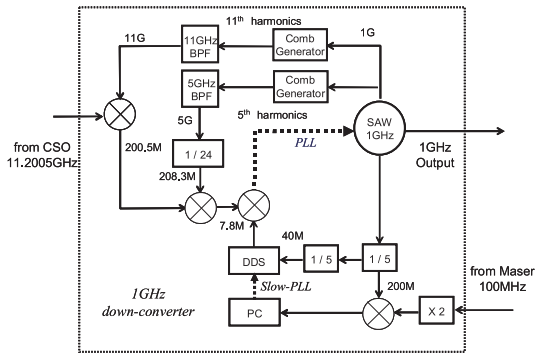

Fig.6 *Block diagram of 1 GHz down-converter*

The intermediate signal (200 MHz) in the down-converter is mixed with a doubled 100 MHz signal from the hydrogen maser in order to compensate the long-term frequency drift dependence of the CSO. The output voltage from the mixer is monitored via an analog to digital converter and the frequency of the DDS is steered to make the output voltage constant over the long-term. By this slow stabilization, the frequency difference between the output signal from the down-converter and the hydrogen maser becomes zero, making it traceable to Japan Standard Time (JST) and International Atomic Time (TAI).

We assembled two nominally identical 1 GHz down-converters to evaluate the performance of the down-converter itself. The 11.2 GHz signal from the CSO is divided into two which are used for phase-locking two 1 GHz down-converters. By varying the frequency of each down-converter's DDS the 1 GHz output signals are independently tunable. Figure 7 shows the residual phase noise spectral density of the down-converter measured with an Agilent E5500 phase noise measurement system, where the 1 GHz signal from one down-converter is used as a signal and the other as a reference. The resultant residual phase noise was measured to be −118 rad^2/Hz at 1 Hz from the carrier and below −140 rad^2/Hz for Fourier frequency beyond 100 Hz. A

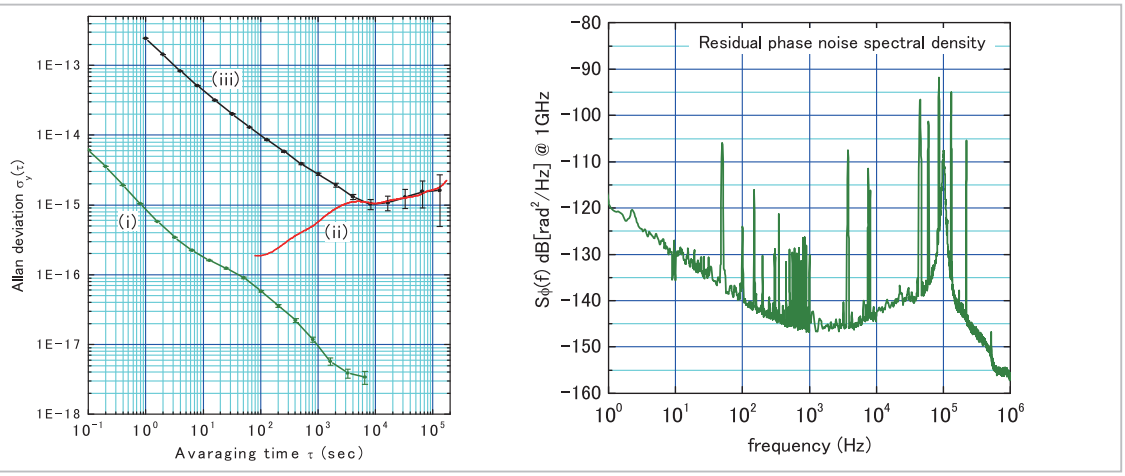

Fig.7 *(Left) Fractional frequency stability of (i) two 1 GHz down-converters without steering to the hydrogen maser, (ii) two 1 GHz down-converters which are loosely locked to two independent masers, (iii) two hydrogen masers. (Right) Residual phase noise density of two identical down-converters at 1 GHz*

peak at around 100 kHz from the carrier is due to the 1 GHz SAW oscillator.

To measure the residual frequency stability of the down-converter, we used an Anritsu Corporation frequency stability measurement system. Both 1 GHz signals are down-converted to 10.1 MHz by mixing with a common reference (989.9 MHz) and the phase difference between two 10.1 MHz signals is measured with high-speed analog to digital converter with a low-pass filter[33]. By this dual-mixing time difference (DMTD) method, we can obtain more reliable results than deducing the stability from the output voltage of a mixer. The residual frequency stability of the 1 GHz down-converters do not degrade the short-term stability of the CSO. The measured stability is better than 1×10^{-15} at an averaging time of 1 second with a measurement bandwidth of 5 Hz.

In addition, a 9.192 GHz microwave signal used for interrogation of the Cs atoms in the NICT cesium fountain CsF-1 has been generated from the down-converted 1 GHz signal. The scheme is depicted in Fig. 8.

In the first stage, the distributed 1 GHz is phase-locked to a 1 GHz SAW oscillator. This tracking filter provides a stable amplitude source for the synthesis chain. The 1 GHz output signal from the SAW oscillator is amplified and injected into a comb generator. The 9th harmonic (9 GHz) of the comb is band-pass filtered and mixed with the 8.992 GHz output from a dielectric resonant oscillator (DRO) to generate 8 MHz. The fine tuning of the up-converter is achieved by controlling a DDS in the chain. This DDS also is modified to take its reference from the 40 MHz reference as described above. The zero beat between the down-converted 8 MHz and 8 MHz output from the DDS is used to digitally phase-lock it to the 8.992 GHz DRO. A portion of 8.992 GHz output is mixed with 200 MHz to generate a 9.192 GHz signal by means of band pass filter. The 9.192 GHz output power is adjustable by varying the 200 MHz signal level via a variable attenuator.

A phase noise of –97 rad^2/Hz at 1 Hz from the carrier was measured, and the short-term frequency stability (shown in Fig. 9) is 1×10^{-15}

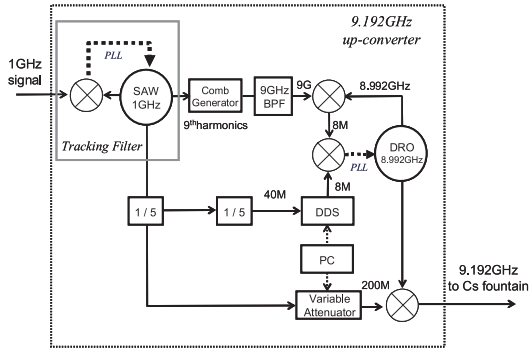

Fig.8 *Block diagram of 9.192 GHz up-converter*

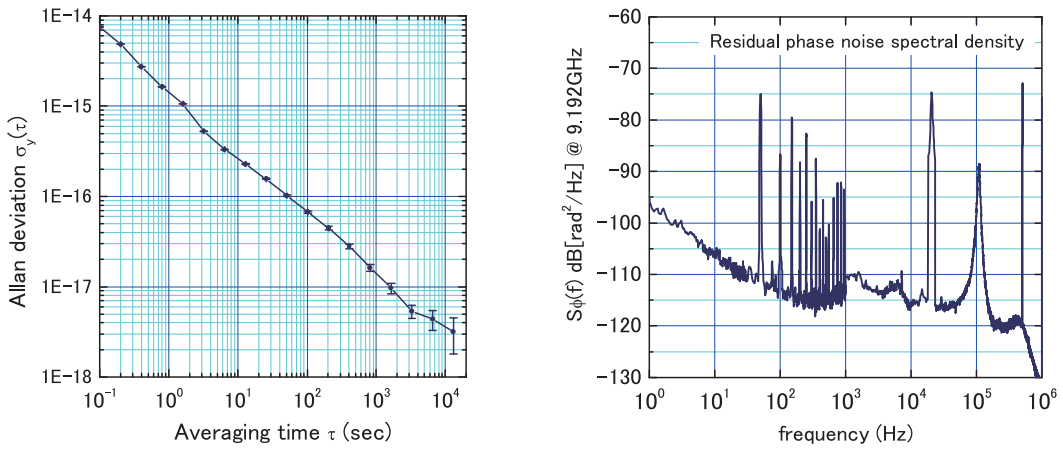

Fig.9 *(Right) Residual phase noise spectral density and (left), residual frequency stability of the 9.192 GHz up-converter*

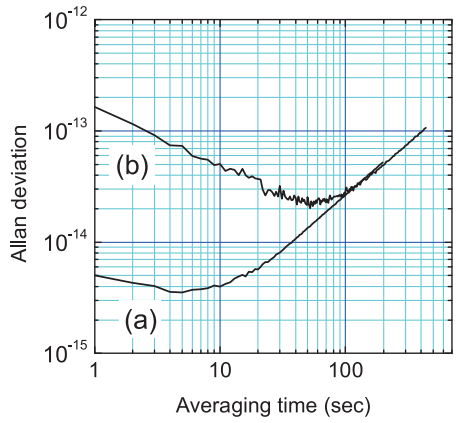

Fig.10 *Fractional frequency stability of 729 nm clock laser by the optical frequency comb based on (a) the CSO and (b) the hydrogen maser*

at an averaging time of 1 second.

We have demonstrated practical realization of the CSO and down-converters described in this article. We have used two optical frequency combs based on femtosecond-pulse mode-locked Ti:sapphire lasers to perform frequency stability measurements of an ultra-narrow linewidth 729 nm clock laser. The repetition rate of the optical comb was phase-locked to the 1 GHz signal derived from either the CSO or the hydrogen maser. Figure 10 shows the results of frequency stability measurements. When the ultra-stable CSO reference was used, a fractional frequency stability of 10^{-15} at 1 second was observed.

5 Conclusion

NICT has introduced a UWA built cryogenic sapphire oscillator with short-term frequency stability better than 2×10^{-15} at 1 second. We have developed synthesis chains to down-convert the 11.2 GHz output frequency of the CSO to 1 GHz signal and to up-convert the resulting 1 GHz signal to 9.192 GHz. The 1 GHz down-converters are loosely locked to the hydrogen masers, which are traceable to Japan Standard Time. An optical comb has been referenced to this highly stable signal and used in stability measurements of a clock laser, and in the near future we will use the CSO signal as a reference for the atomic fountain NICT-CsF1.

Acknowledgements

The authors wish to acknowledge past and present members of the Frequency Standards and Metrology Research Group at UWA; A.N. Luiten, S. Chang and A. Mann, P.L. Stanwix, M.E. Tobar, J.G. Hartnett and E.N. Ivanov.

References

1 M. Kumagai, H. Ito, M. Kajita, and M. Hosokawa, "Evaluation of caesium atomic fountain NICT-CsF1," Metrologia, Vol. 45, pp. 139–148, 2008.

2 S. Nagano, H. Ito, Y. Li, K. Matsubara, and M. Hosokawa, "Stable Operation of Femtosecond Laser Frequency Combs with Uncertainty at the 10^{-17} Level toward Optical Frequency Standards," Jpn. J. Appl. Phys., Vol. 48, No. 042301, pp. 1–8, 2009.

3 V. B. Braginsky, V. P. Mitrofanov, and V. I. Panov, "Systems with Small Dissipation," University of Chicago Press, 1985.

4 A. G. Mann, "Frequency Measurement and Control: Advanced Techniques and Future Trends, edited by A. N. Luiten," Springer, pp. 37–66, 2001.

5 A. J. Giles, A. G. Mann, S. K. Jones, D. G. Blair, and M. J. Buckingham, "A very high stability sapphire loaded superconducting cavity oscillator," Physica B, Vol. 165, pp. 145–146, 1990.

6 A. N. Luiten, A. G. Mann, and D. G. Blair, "Power stabilized cryogenic sapphire oscillator," IEEE Trans. Instrum. Meas., Vol. 44, pp. 132–135, 1995.

7 See http://www.crystalsystems.com/hemex_sapph.html

8 G. Santarelli, Ph. Laurent, P. Lemonde, A. Clairon, A. G. Mann, S. Chang, A. N. Luiten, and C. Salomon, "Quantum Projection Noise in an Atomic Fountain: A High Stability Cesium Frequency Standard," Phys. Rev. Lett., Vol. 82, pp. 4619–4622, 1999.
9 P. Wolf, S. Bize, A. Clairon, A. N. Luiten, and G. Santarelli, "Tests of Lorentz Invariance using a Microwave Resonator," Phys. Rev.Lett., Vol. 90, No. 060402, pp. 1–4, 2003.
10 P. Lemonde, P. Laurent, E. Simon, G. Santarelli, A. Clairon, C. Salomon, N. Dimarcq, and P. Petit, "Test of a cold atom clock prototype in absence of gravity," IEEE Trans. Instrum. Meas., Vol. 48, pp. 512–515, 1999.
11 J. G. Hartnett, C. R. Locke, E. N. Ivanov, M. E. Tobar, and P. L. Stanwix, "Cryogenic sapphire oscillator with exceptionally high long-term frequency stability," Appl. Phys. Lett., Vol. 89, No. 203513, pp. 1–3, 2006.
12 M. E. Tobar, E. N. Ivanov, C. R. Locke, J. G. Hartnett, and D. Cros, "Improving the frequency stability of microwave oscillators by utilizing the dual-mode sapphire loaded cavity resonator," Meas. Sci. Technol., Vol. 30, pp. 1284–1288, 2002.
13 M. E. Tobar, G. L. Hamilton, E. N. Ivanov, and J. G. Hartnett, "New Method to Build a High Stability Sapphire Oscillator from the Temperature Compensation of the Difference Frequency Between Modes of Orthogonal Polarization," IEEE Trans. Ultrason. Ferroelectr. Freq. Control, Vol. 50, pp. 214–219, 2003.
14 J. G. Hartnett, M. E. Tobar, and J. Krupka, "Complex paramagnetic susceptibility in titanium-doped sapphire at microwave frequencies," J. Phys. D, Vol. 34, pp. 959–967, 2001.
15 J. G. Hartnett and M. E. Tobar, "Frequency Measurement and Control: Advanced Techniques and Future Trends edited by A. N. Luiten," Springer, pp. 67–79, 2001.
16 J. G. Hartnett, M. E. Tobar, A. G. Mann, E. N. Ivanov, J. Krupka, and R. Geyer, "Frequency-temperature compensation in Ti^{3+} and Ti^{4+} doped sapphire whispering gallery mode resonators," IEEE Trans. Ultrason. Ferroelectr. Freq. Control, Vol. 46, pp. 993–1000, 1999.
17 J. Millo, R. Boudot, M. Lours, P. Y. Bourgeois, A. N. Luiten, Y. Le Coq, Y. Kersalé, and G. Santarelli, "Ultra-low-noise microwave extraction from fiber-based optical frequency comb," Optics Letters, Vol. 34, No. 23. pp. 3707–3709, 2009.
18 Y. Le Coq, J. Millo, W. Zhang, M. Abgrall, M. Lours, H. Jiang, E.M.L. English, R. Boudot, P.Y. Bourgeois, M.E. Tobar, J. Guena, A. Clairon, S. Bize, A.N. Luiten, Y. Kersale, and G. Santarelli, "Ultra-low noise microwave generation using femtosecond lasers and applications," 2010 Conference on Lasers and Electro-Optics (CLEO) and Quantum Electronics and Laser Science Conference (QELS), pp. 1–2, 2010.
19 D. Chambon, S. Bize, M. Lours, F. Narbonneau, H. Marion, A. Clairon, G. Santarelli, A. Luiten, and M. Tobar, "Design and Realization of a Flywheel Oscillator for Advanced Time and Frequency Metrology," Rev. Sci. Instrum., Vol. 76, No. 094704, pp. 1–5, 2005.
20 D. Chambon, M. Lours, F. Chaplet, S. Bize, M. Tobar A. Clairon, and G. Santarelli, "Design and Metrological Features of Microwave Synthesizers for Atomic Fountain Frequency Standard," IEEE Trans. Instrum. Meas., Vol. 54, pp. 729–735, 2007.
21 O. Lopez, A. Amy-Klein, C. Daussy, C. Chardonnet, F. Narbonneau, M. Lours, and G. Santarelli, "86-km optical link with a resolution of 2×10^{-18} for RF frequency transfer," Eur. Phys. J. D., Vol. 48, pp. 35–41, 2008.
22 M. Fujieda, M. Kumagai, T. Gotoh, and M. Hosokawa, "Ultrastable Frequency Dissemination via Optical Fiber at NICT," IEEE Trans. Instrum. Meas., Vol. 58, pp. 1223–1228, 2009.
23 L. Rayleigh, "The problem of the whispering gallery," Philos. Mag., Vol. 20, pp. 1001–1004, 1910.

24 M. E. Tobar and D. G. Blair, “A generalized equivalent circuit applied to a tunable sapphire-loaded superconducting cavity,” IEEE Trans. Microwave Theory Tech., Vol. 39, pp. 1582–1594, 1991.
25 M. E. Tobar, “Effects of spurious modes in resonant cavities,” J. Phys. D, Vol. 26, pp. 2022–2029, 1993.
26 S. Chang, A. Mann, and A. Luiten, “Improved cryogenic sapphire oscillator with exceptionally high frequency stability,” Electron. Lett. Vol. 36, pp. 480–481, 2000.
27 S. Chang, A. Mann, and A. Luiten, “Improved cryogenic sapphire oscillator with exceptionally high frequency stability,” Electron. Lett., Vol. 36, pp. 480–481, 2000.
28 R. V. Pound, “Electronic Frequency Stabilization of Microwave Oscillators,” Rev. Sci. Instrum., Vol. 17, pp. 490–505, 1946.
29 R. W. P. Drever, J. L. Hall, F. V. Kowalski, J. Hough, G. M. Ford, A. J. Munley, and H. Ward, “Laser phase and frequency stabilization using an optical resonator,” Appl. Phys. B, Vol. 31, pp. 97–105, 1983.
30 S. Chang, A. G. Mann, A. N. Luiten, and D. G. Blair, “Measurements of Radiation Pressure Effect in Cryogenic Sapphire Dielectric Resonators,” Phys. Rev. Lett., Vol. 79, pp. 2141–2144, 1997.
31 J. D. Anstie, J. G. Hartnett, M. E. Tobar, E. N. Ivanov, and P. L. Stanwix, “Second generation 50 K dual-mode sapphire oscillator,” IEEE Trans. Ultrason. Ferroelectr. Freq. Control, Vol. 53, pp. 284–288, 2006.
32 C.R. Locke, E. N. Ivanov, J. G. Hartnett, P. L. Stanwix, and M. E. Tobar, “Invited Article: Design techniques and noise properties of ultrastable cryogenically cooled sapphire-dielectric resonator oscillators,” Rev. Sci. Instrum., Vol. 79, No. 051301, pp. 1–12, 2008.
33 K. Mochizuki, M. Uchino, and T. Morikawa, “Frequency-Stability Measurement System Using High-Speed ADCs and Digital Signal Processing,” IEEE Trans. Instrum. Meas., Vol. 56, pp. 1887–1893, 2007.

(Accepted Oct. 28, 2010)

Clayton R. Locke, *Ph.D.*

Invited Executive Researcher, Space-Time Standards Group, New Generation Network Research Center

Optical Frequency Standards, Space-Time Measurements

KUMAGAI Motohiro, *Ph.D.*

Senior Researcher, Space-Time Standards Group, New Generation Network Research Center

Atomic Frequency Standard, Frequency Transfer using Optical Fibers

ITO Hiroyuki, *Ph.D.*

Senior Researcher, Space-Time Standards Group, New Generation Network Research Center

Atomic Frequency Standard, Optical Frequency Standards

NAGANO Shigeo, *Ph.D.*

Senior Researcher, Space-Time Standards Group, New Generation Network Research Center

Optical Frequency Standards, Space-Time Measurements

John G. Hartnett, *Ph.D.*

Professor, School of Physics, University of Western Australia

Microwave Frequency Standards, Space Time Measurement

Giorgio Santarelli

LNE-SYRTE, Observatoire de Paris

HOSOKAWA Mizuhiko, *Ph.D.*

Executive Director, New Generation Network Research Center

Atomic Frequency Standards, Space-Time Measurements